



Is sulfur-doped TiO_2 an effective visible light photocatalyst for remediation?

Erin M. Rockafellow, Laine K. Stewart, William S. Jenks *

Department of Chemistry, Iowa State University, Ames, IA 50011-3111, United States

ARTICLE INFO

Article history:

Received 20 January 2009

Received in revised form 18 June 2009

Accepted 22 June 2009

Available online 30 June 2009

Keywords:

Photocatalysis

Doped titanium dioxide

Visible light

ABSTRACT

Doping titania with main group elements increases the visible light absorbance by introducing a localized band of orbitals within the band gap, but the effect of such dopants on the oxidizing power of the catalysts remains ambiguous. Three aromatic organic probe molecules – 4-methoxyresorcinol, quinoline, and 1-(*p*-anisyl)neopentanol – have been used to evaluate the oxidative chemistry of S-doped TiO_2 and test the efficacy of the catalyst with visible irradiation. With visible irradiation, a phenol is degraded efficiently, apparently through absorption by a CT band. For the other two probes, the most straightforward interpretation is that visible irradiation does not produce hydroxyl-type chemistry, but can accomplish single-electron transfers in favorable cases. The utility of sulfur-doped TiO_2 as a photocatalyst over undoped titania depends entirely whether the requirement for visible-light functionality, even if at low efficiency, outweighs a modest drop in the efficiency of catalysis using UV light.

© 2009 Elsevier B.V. All rights reserved.

1. Introduction

The use of titanium dioxide as a photocatalyst for the degradation of organic compounds in water has received a great deal of attention [1–3]. Titanium dioxide is of particular interest because it is robust, thermally stable, non-toxic, and cheap. Upon absorption of light with sufficient energy for band gap excitation, charge separation occurs, promoting an electron (e^-) to the conduction band leaving a void, or hole (h^+), in the valence band. These photogenerated charges can migrate to the surface of the photocatalyst where charge transfer with surface-bound adsorbates and nearby molecules can occur in competition with recombination of the electron/hole pair. Nearby organic molecules can then undergo oxidative reactions by either indirect, hydroxyl-like pathways (hereafter referred to as $\text{HO}^{\bullet}_{\text{ads}}$ to distinguish this chemistry from that of true bulk-solvated hydroxyl radicals, HO^{\bullet}) or single electron transfer (SET), which involves direct electron transfer from the organic molecule to the photogenerated hole (“hole attack”) or potentially to another photogenerated reactive species, like HO^{\bullet} [3–7].

Unfortunately, anatase, which is believed to be the most reactive phase of TiO_2 , has a low quantum yield for oxidation steps ($\leq 5\%$) as a result of rapid recombination of photogenerated charges. In addition, pure anatase is only able to use $< 10\%$ of the terrestrial solar spectrum because of its wide band gap (3.2 eV),

with rutile having a slightly smaller band gap (3.0 eV), but generally lower activity.

Doping TiO_2 with metal cations or main group elements has been shown to induce extensions of the absorption spectrum into the visible [3,8,9]. Although transition metals give the desired red shift, many of them can act as recombination centers. This reduces the semiconductor's photochemical efficiency and therefore utility as a photocatalyst [3,5]. Recent research has focused greatly on doping TiO_2 with nonmetal main group elements to create materials we designate as N- TiO_2 , C- TiO_2 , etc., with S- TiO_2 being the focus of this paper [8,10–17].

Understanding the origin of the shifted absorption and its relationship to the photocatalytic chemistry is essential. Asahi originally proposed that nitrogen doping creates a delocalized mixing between the O 2p and N 2p orbitals causing a rise in the valence band [8]. Most current research supports an alternative proposal in which the dopant atom orbitals generate an isolated mid-gap level above the valence band [7,12,18,19]. Intuitively, this point is a key one for understanding the chemistry that these catalysts will initiate, given that oxidation is the main TiO_2 -mediated degradation pathway. Raising the bulk valence band energy level would necessarily lower the oxidizing power of the photochemically generated hole and potentially interfere with certain reactions the pristine catalyst could perform. The role of isolated mid-gap level holes is less clear, though they also should result in low energy “hole traps” that were less chemically active than the main valence band holes. Excitation in the low energy edge of the absorption would presumably mean direct formation of such trapped holes, but UV excitation could also lead to low energy

* Corresponding author. Tel.: +1 5152944711; fax: +1 5152949623.

E-mail address: wsjenks@iastate.edu (W.S. Jenks).

trapped holes via migration to the dopant center. It is thus apparent that at the limit of high charge mobility and rapid trapping, all excitations might have a lowered oxidation power over the undoped TiO_2 . On the other hand, if oxidation of adsorbed substrates were competitive with charge migration within the particle, a wavelength dependence on the observed chemistry might be found.

Several key studies have reported on the differences in charge carrier mobility generated by irradiation with UV light versus visible light [7,17,19,20]. Others have recently noted wavelength-dependent chemistry for N- TiO_2 remediation of ethylene glycol in acetonitrile [19], as well as C- TiO_2 -mediated degradation of molecules with different binding abilities and oxidation potentials [7].

To probe the photocatalytic activity of doped titania, many other studies have used dyes as chemical probes, some of which are prone to both oxidative and reductive degradation pathways and are often unrepresentatively easy to oxidize or reduce, compared to more common relevant pollutants. Dyes also absorb light in the visible region, which is an undesirable trait. The use of methylene blue, perhaps the most common of these, remains controversial for these and other reasons [16,21]. We prefer molecules more closely related to common pollutants such as aromatic pesticides, herbicides, manufacturing byproducts, or petroleum products that also have well-defined oxidative pathways [2,22,23].

In this paper, we report an investigation of S- TiO_2 prepared in two ways – a conventional sol-gel preparation [13,14], and a modification of existing TiO_2 by annealing with S_8 – and an evaluation of the chemical reactivity of these catalysts in the UV and visible ranges. As chemical probes, we use three aromatic molecules with considerably different adsorption modes and modes of reactivity. These compounds, 4-methoxyresorcinol (MR, 4-methoxybenzene-1,3-diol), 1-(*p*-anisyl)neopentanol (AN, 1-(4-methoxyphenyl)-2,2-dimethylpropan-1-ol), quinoline (Q), have well established patterns of oxidative reactivity [6,22,24–26]. By examining the partial degradation mixtures at low conversion of the starting material, reaction products can be used to distinguish between hydroxyl-type and single-electron transfer (SET) interactions with the catalyst, as shown in Scheme 1.

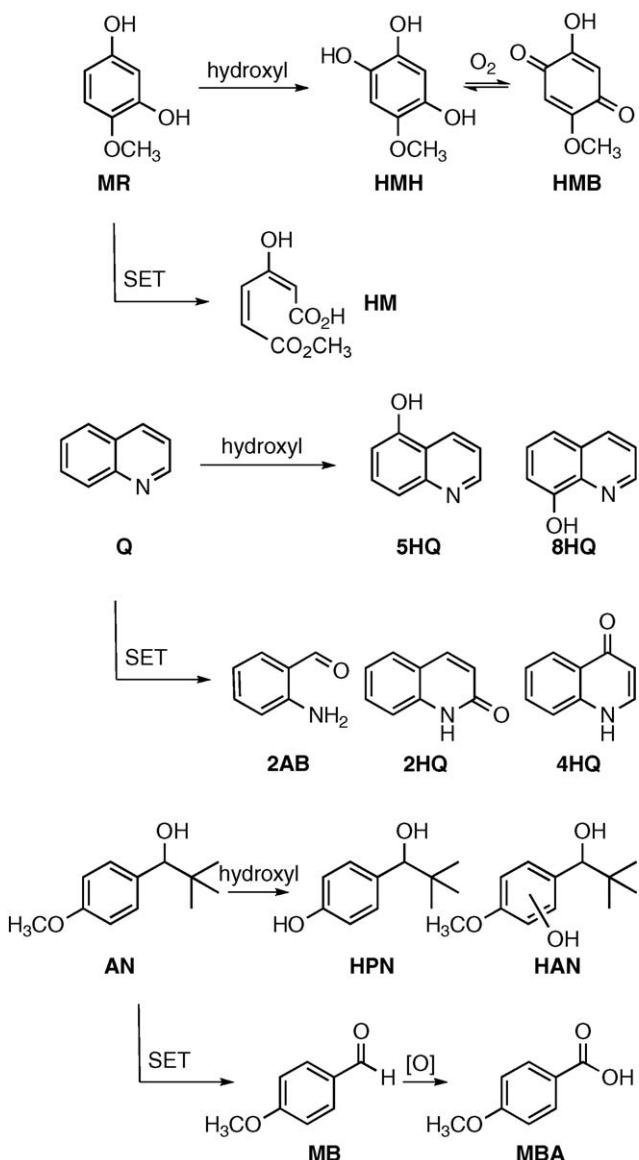
2. Experimental section

2.1. Materials

Chemicals were purchased at the highest available purity and used as received, unless noted otherwise. 4-Methoxyresorcinol [27] and 1-(*p*-anisyl)neopentanol [24] were prepared by literature methods. Water was purified using a Milli-Q UV plus system with a resistivity above 18 $\text{M}\Omega\text{cm}$. PC500, a commercial anatase, was received from Millenium Chemical Company, and used only for the purpose of showing the anatase pattern in the powder XRD.

2.2. Photocatalyst preparation

Sulfur-doped titanium dioxide (S- TiO_2) was prepared using a lightly modified literature procedure due to Ohno [13,14]. Thiourea (53.4 g) was dissolved in 550 mL 90% ethanol followed by drop-wise addition of titanium (IV) isopropoxide (51.5 mL) and vigorous stirring to yield a white precipitate. The solution was stirred at room temperature under aerated conditions for 48 h to allow for complete hydrolysis. Solvent was removed under reduced pressure, and the remaining white powder was annealed at 450 °C for 4 h. The material was then washed thoroughly with water to remove residual surface adsorbates and any surface



Scheme 1. Early photocatalytic degradation steps for MR, Q, and AN.

sulfates. S- TiO_2 was obtained as a vivid yellow powder. Undoped TiO_2 was prepared by a similar method as S- TiO_2 without thiourea.

A second method was also used for the synthesis of sulfur-doped titanium dioxide, designated $\text{S}_8\text{-TiO}_2$. Samples of undoped TiO_2 obtained from the previous procedure were used as the starting material. Undoped (but otherwise identically prepared) unannealed, amorphous TiO_2 (5.00 g) and S_8 (2.00 g) were mixed and ground together thoroughly with a mortar and pestle, followed by annealing at 350 °C for 4 h. (The boiling point of S_8 is 445 °C). The resulting grayish-tan powder was washed with water to remove surface adsorbates and sulfates. As a control, washing with CS_2 , done to wash away any residual S_8 or related materials, was also performed, and no color change resulted.

2.3. Catalyst characterization

Powder X-ray diffraction (XRD) spectra were taken with X-ray powder diffractometer employing $\text{Cu K}\alpha$ radiation. Surface analysis of the materials was performed by nitrogen sorption isotherms in a sorptometer. The surface areas were calculated by the Brunauer–Emmett–Teller (BET) method. X-ray photoelectron spectroscopy

(XPS) was done using a multitechnique spectrometer utilizing nonmonochromatized Al K radiation with a 1 mm^2 sampling area. The take off angle was fixed at 45° . Spectra were calibrated to the C1s peak at 284.7 eV. Diffuse reflectance spectra (DRS) were generated with a UV-vis spectrometer equipped with a diffuse reflectance accessory. MgO was used as a background reference. For transmission electron microscopy (TEM) measurements, an aliquot of the powder was sonicated in nanopure water for 15 min. A single drop of this suspension was placed on a lacey carbon coated copper TEM grid and dried in air. The TEM examination was completed on an electron microscope operated at 200 kV to examine at electron optical magnification of 64,000 to 550,000.

2.4. Photocatalytic measurements

Reaction mixture preparation, photolysis conditions, and analysis procedures were similar to previous work [28]. The suspensions contained doped or undoped titania at 1.00 mg/mL. The initial concentrations of probe molecules and solution pH values were as follows: 1.0 mM MR at pH 8.5 ± 0.5 , 0.3 mM AN at pH 8.5 ± 0.5 , 0.15 mM quinoline at pH 6.0 ± 0.5 or pH 3.0 ± 0.5 . The pH was adjusted and maintained over the photolysis by careful addition of aqueous NaOH or HNO₃. The solution was purged with O₂ and stirred in the dark for a minimum of 30 min before reactions. Reactions were irradiated with 350 nm broad range 4 W bulbs in a Rayonet minireactor or light from 75 W Xe arc lamp passed through a water filter and a 495 nm longpass filter. Potassium ferrioxalate was used as a chemical actinometer [29]. All reactions were carried out at ambient temperature with continuous stirring and O₂ bubbling.

For kinetics, 1 mL samples were acidified, centrifuged, filtered and analyzed by HPLC. HPLC analysis was done using a C18 reverse phase column using a diode array detector. Compounds were identified by comparison to authentic samples. MR degradation analysis was performed using 70% water containing 0.2% acetic acid and 30% methanol as the eluent at 1 mL/min and monitored at 290 nm. The eluent used for analysis of AN was 70% acetonitrile and 30% water at 1 mL/min and detected at 270 nm. Quinoline and the oxidized products were easily identifiable by HPLC. However, it was determined that using two different mobile phases was ideal for analysis of all the products, as there were some difficulties with overlap. For HPLC analysis of quinoline, 4-quinolinone (4HQ), 2-aminobenzaldehyde (2AB), and 2-quinolinone (2HQ), the solvent was 1:3 methanol:water with 0.2% acetic acid. Flow was 0.9 mL/min and traces were monitored at 230 nm and 325 nm. Analysis of 5-hydroxyquinoline (5HQ) and 8-hydroxyquinoline (8HQ) was done using 1:9 methanol:water with 0.2% acetic acid as the mobile phase with an elution rate of 0.75 mL/min and monitoring at 250 nm.

For product analysis for MR and AN degradations, GC-MS (or routine GC) was used and compounds were verified by comparison to authentic samples. Approximately 60 mL of the irradiated solution was acidified, centrifuged and filtered. Fifty mL of the filtrate was concentrated by evaporation under reduced pressure until 3–5 mL remained, which was then freeze-dried. For GC-MS analysis of MR reactions, 1 mL of a 0.5 mM dodecane in pyridine stock solution was added to the residual solid followed by silylation as previously described [25,28]. For GC-MS analysis of AN reactions, the lyophilized solid was dissolved in 0.5 mL methanol containing 0.5 mM dodecane, followed by agitation and centrifugation. GC-MS was done by GC-TOF analysis with a 30 m DB-5 column.

3. Results

3.1. Physical characterization of catalysts

Powder diffraction data revealed that the prepared materials were anatase (Fig. 1). The average crystallite size of S-TiO₂, S₈-TiO₂

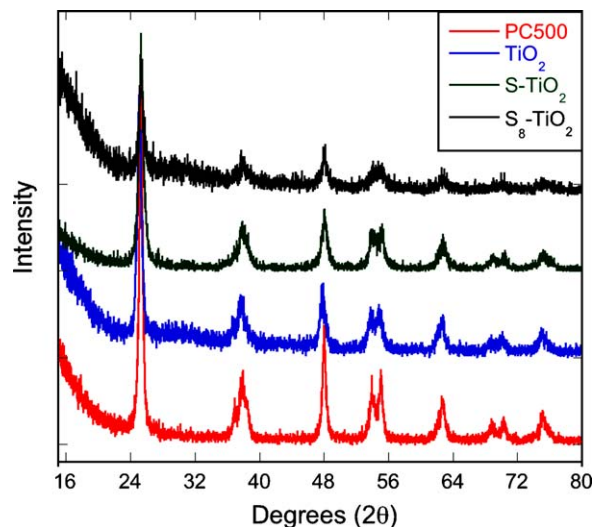


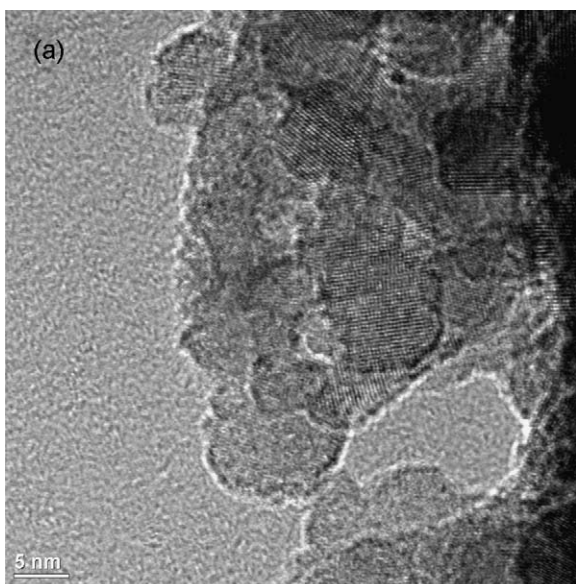
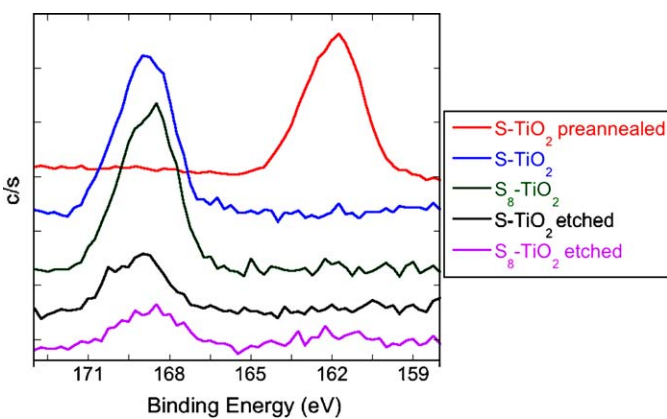
Fig. 1. XRD of synthesized S-TiO₂ and TiO₂ compared to commercially available anatase (PC500).

and undoped TiO₂ were 13 nm, 13 nm, and 14 nm calculated using the Scherrer formula ($d = 0.9\lambda/\beta_{1/2}\cos\theta$). These values are consistent with the typical particle sizes of 5–15 nm observed in the transmission electron microscopy images (Fig. 2). The BET surface was 93 m²/g for S-TiO₂ and 69 m²/g for undoped TiO₂.

Fig. 3 shows the XP spectra of the S 2p region obtained under different conditions. The spectrum obtained from a dried, but unannealed sample has a peak at 162 eV, which corresponds to S²⁻. The spectra also indicated the presence of carbon and nitrogen derived from thiourea. After annealing, the 162 eV S²⁻ peak disappears and is replaced by a new one at 169 eV, indicating the presence of an S⁴⁺ and/or S⁶⁺ species [30]. Etching, which removes the first few atomic surface layers, reduced the signal strength by a factor of 2. In post-annealing spectra, no peaks corresponding to nitrogen were observed, and no carbon peaks were observed, outside of the ubiquitous carbon C 1s peak corresponding to adventitious/ambient carbon. By XPS, the total sulfur concentration was 0.8% (S-TiO₂) or 1.0% (S₈-TiO₂), determined before etching. In the S₈-TiO₂ sample, a small peak at 162 eV appears after etching, demonstrating the presence of S²⁻. Diffuse reflectance data show that sulfur doping causes a significant red shift relative to the undoped titania prepared without the sulfur source (Fig. 4).

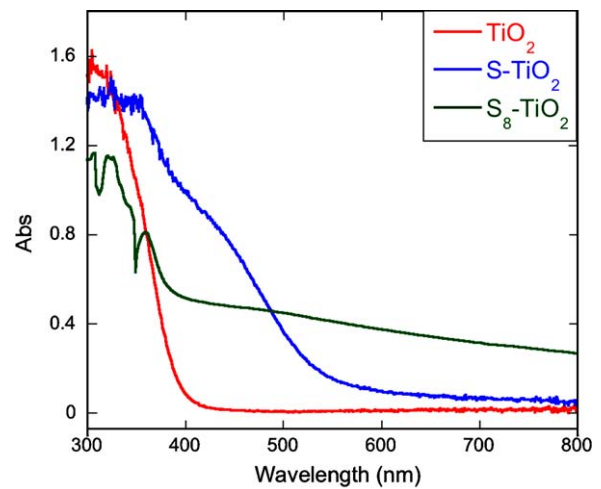
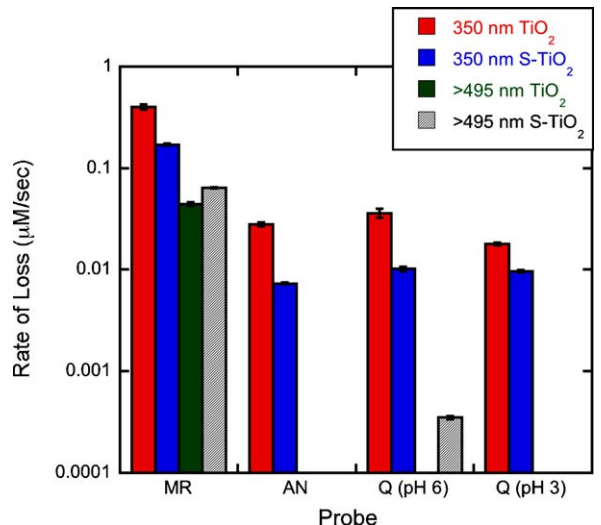
3.2. Photocatalytic degradations

Fig. 5 shows the initial zero-order rates of loss on a logarithmic scale for photocatalytic degradation of the probe molecules. The S₈-TiO₂ behaved very similarly to S-TiO₂ in all tested cases. Control experiments showed that the organic compounds were stable under the conditions in the dark on the time scale of all reactions. Rates were normalized with actinometry from one light source to the other to account for varying photonic flux [31]. The light sources were fluorescent tubes with broad irradiation centered at 350 nm and a Xe arc lamp filtered through water (to remove excessive IR) and at 495 nm longpass filter. Thus, the latter is an exclusively visible (and IR) light source, while the former is fully in the UV. According to Fig. 4, the undoped TiO₂, in the absence of any organic substrate, should not absorb any light from the >495 nm source, and such irradiation is also near the red edge of absorption for the doped catalyst. Under UV irradiation, the pristine TiO₂ degraded the probe compounds more rapidly than did S-TiO₂, by factors of approximately 2.

Fig. 2. TEM images of (a) TiO_2 and (b) S-TiO_2 .Fig. 3. XP spectra of S-TiO_2 .

3.2.1. Rates of degradation

MR was degraded faster than either of the other two probe molecules, regardless of conditions (Fig. 5). Perhaps most interesting is the observation that MR is degraded at comparable

Fig. 4. Diffuse reflectance spectra of undoped TiO_2 and S-TiO_2 .Fig. 5. Comparison of probe molecule degradation rates for TiO_2 and S-TiO_2 photocatalytic degradation under UV and visible light. Rates are normalized for variances in light output using ferrioxalate actinometry.

rates when the naked catalyst does not absorb the light. Given that MR is an electron rich phenol, the most probable explanation is the formation of a charge transfer complex between it and TiO_2 , which is irradiated even in the visible. The suspensions were not visibly colored, but the concentration of MR is sufficiently low that such obvious coloration is not expected. This type of CT complex has been documented in related molecules before [32,33]. Rates alone do not distinguish whether the >495 nm-initiated degradation with S-TiO_2 were based on the same CT interaction or on the visible absorption of the catalyst.

The rate of degradation of AN mediated by any of the catalysts under UV illumination is an order of magnitude lower than the rate of loss of MR. The rate for S-TiO_2 is smaller than that for TiO_2 by a factor of about 2.5, both under 350 nm irradiation. Over the course of 48 h of irradiation (which was the practical limit for keeping the dark concentration the same within a few percent), no loss of AN was detectable when using >495 nm irradiation, regardless of the catalyst.

Q was degraded efficiently with UV light, similarly to the other two probes, at either pH 3 or 6 by both S-TiO_2 and $\text{S}_8\text{-TiO}_2$. Fig. 6 shows the full set of kinetic data for degradation of Q using S-TiO_2 . $\text{S}_8\text{-TiO}_2$ removes quinoline approximately 2.5 times faster than S-TiO_2 .

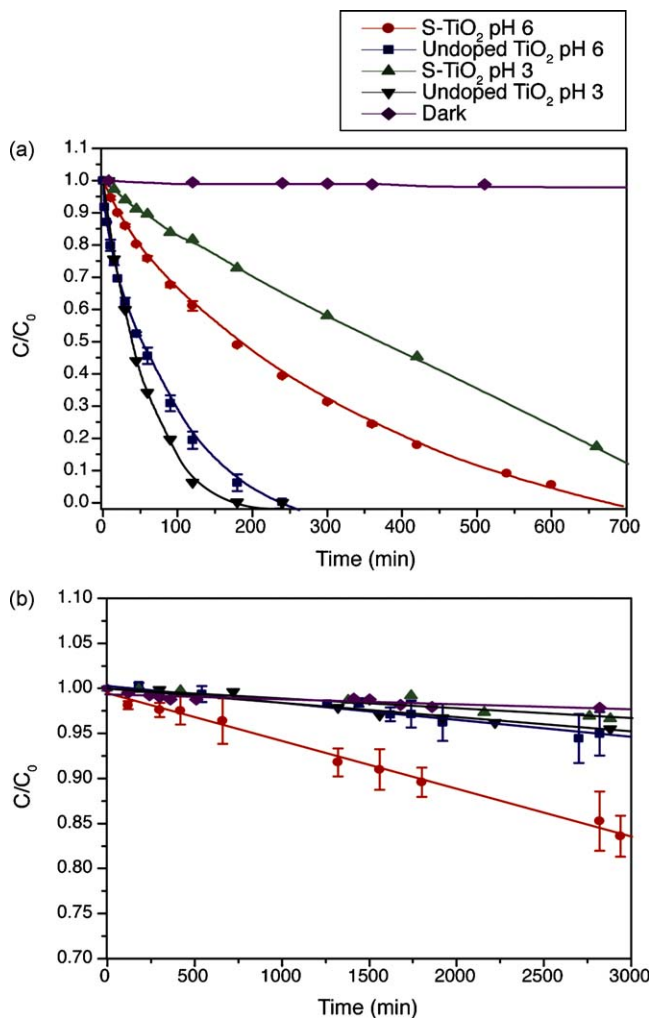


Fig. 6. Heterogeneous photocatalytic degradation of quinoline under (a) 350 nm and (b) ≥ 495 nm.

TiO₂ at pH 3, and 1.5 times faster at pH 6. Like AN, loss of Q when using TiO₂ and visible irradiation was not distinguishable from the dark background. This same result was obtained when S-TiO₂ or S₈-TiO₂ was used as the photocatalyst at pH 3 under >495 nm irradiation. However, at pH 6, Q was reproducibly degraded at a normalized rate about two orders of magnitude more slowly than under UV irradiation (15% in 48 h) by S-TiO₂ and wavelengths >495 nm. However, since the fraction of absorbed photons is not known, but is very likely lower for the visible irradiations, this should be taken as a lower limit of the relative rates and not an absolute ratio.

3.2.2. Product analysis

Product analysis at fixed low conversion can provide useful, if qualitative, information about the relative rates of formation of initial degradation products. The major concern is the secondary consumption of the intermediates; in extreme cases, no intermediates are observed at all because they are consumed much more rapidly than they are formed. However, the present compounds were chosen in large part because their early degradation products are observable and chemically interpretable. An admittedly simplified scheme for each molecule, based on previous studies, is given in **Scheme 1**. A few of these products clearly require more than one step (e.g., MBA, which is undoubtedly secondary to MB). Hydroxymethoxy hydroquinone (HMH) spontaneously oxidizes to the quinone in aerated water on

Table 1
Ratios of early degradation intermediate products.

Probe molecule	Observed SET:HO [•] _{ads} intermediate product ratio ^a			
	TiO ₂		S-TiO ₂	
	UV	Visible	UV	Visible
4-Methoxyresorcinol (MR) ^b	1.3	1.7	1.2	1.2
p-Anisyl-1-neopentanol (AN) ^b	0.9 ^c	–	0.1	–
Quinoline (Q) (pH 6)	4.2	–	6.2	SET only
Quinoline (Q) (pH 3)	0.2 ^d	– ^d	0.04	– ^d

^a MR and AN product ratios were found using GC peak areas relative to dodecane as an internal standard. Q product ratios were found by concentrations based on HPLC peak areas versus standard calibrations.

^b pH 8.5 \pm 0.5.

^c Peak areas in the GC trace were very small, indicating intermediate products may be consumed faster than the parent probe molecule.

^d Trace amounts of 5HQ were observed.

handling, although the reverse reaction [34] almost certainly takes place with the light on.

Table 1 summarizes the results of product studies for all the probes and catalysts for low conversion, with the products grouped together as indicating hydroxyl-like chemistry or SET-initiated chemistry, as indicated in **Scheme 1**. The ratios given in **Table 1** for MR show there is a slight excess of SET products over HO[•]_{ads} products, but both pathways are competitive. Moving from UV to visible, the product yield shifts for TiO₂, but does not do so for S-TiO₂.

For AN, no products were observed for the visible irradiations, as indicated by the kinetics experiments. For this poorly binding substrate, when UV irradiation at pH 8.5 was used, hydroxyl products predominate only slightly in the undoped TiO₂, but quite strongly when S-TiO₂ is the catalyst. (This latter result was also our observation using commercially available anatase catalysts [22].) The product peaks were smaller than expected, implying that even at modest degradation of the parent compound, secondary degradation reactions were important. This phenomenon is not particularly surprising for poorly binding substrates; the more oxidized products may more easily be adsorbed to the catalyst.

Degradations were carried out at pH 3 and 6 for quinoline, which is below and above the pKa of quinolinium ion, respectively. Traces showing the product evolution as a function of irradiation time for quinoline, using TiO₂ as the catalyst, are given in **Fig. 7**. **Fig. 8** shows the same data for quinoline and S-TiO₂, including the >495 nm photolyses. S₈-TiO₂ behaved in the same manner as S-TiO₂ in >495 nm degradations of quinoline at both pH 3 and 6.

With UV exposure, the SET products were favored by a slightly larger margin with the sulfur-doped catalyst, compared to the undoped. A dramatic difference in the absolute ratio is seen for the quinoline (pH 6) vs. quinolinium (pH 3) case (**Figs. 7 and 8**). Intermediate product studies after 2 h of irradiation reveal that S₈-TiO₂ favored SET products by more than 10:1 at pH 6 and hydroxyl products by more than 23:1 at pH 3. In general, the favoring of SET products at pH 6 is very likely due to superior adsorption of the neutral compound through the nitrogen lone pair, favoring SET as a mechanism [6].

These results are consistent with those obtained by the Pichat group using P25 as the photocatalyst [6]. However, Pichat reports 2AB as the major product, in contrast to the current observations. We were able to reproduce the Pichat result by using P25 as a photocatalyst instead of the pure anatase used in this study. Thus the internal change within the SET product distribution is attributable to differences in the catalyst.

A measurable difference in degradation rate of Q by S-TiO₂ and S₈-TiO₂ using UV light was observed, i.e., the latter provided faster removal by a factor of 2.5 at pH 3 and 1.5 at pH 6, and a rate closer to that of the undoped TiO₂. We presume (but cannot prove) that

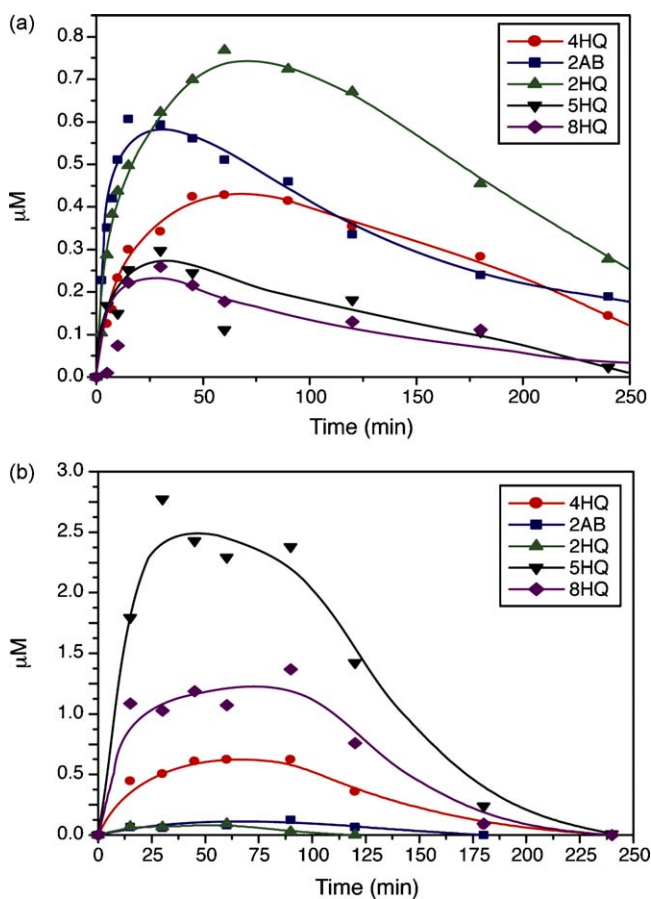


Fig. 7. Intermediate products formed from the TiO_2 -mediated degradation of quinoline at (a) pH 6 and (b) pH 3.

the $\text{S}_8\text{-TiO}_2$ has its sulfur localized in the several outer layers of the catalyst. If so, we may speculate that the sulfur sites that are throughout the interior of the S-TiO_2 do not contribute to the degradation in any useful way, but may represent recombination centers that lower the overall efficiency.

With visible photolysis of Q, there was a dramatic difference between the catalysts. The undoped TiO_2 did not catalyze any degradation as detected by kinetics at pH 6, but S-TiO_2 did, with the products being entirely SET-derived. Despite the loss of Q being indistinguishable from dark reaction at pH 3, trace amounts of 5HQ could be detected.

Additional control experiments were done to determine if slightly higher energy visible light could be used to generate hydroxyl chemistry. Quinolinium degradation at pH 3 was the probe of choice for this. Instead of using 495 nm cutoff filters, two sets of otherwise identical experiments were carried out at pH 3, using 435 nm and 455 nm cutoff filters, respectively. As shown in Fig. 4, these cutoff wavelengths are both longer than the classical absorption of the TiO_2 . Also, as a negative control, undoped TiO_2 was examined under the same conditions. The results for all three cutoffs (435 nm, 455 nm, and 495 nm) were the same within experimental uncertainty, i.e., no hydroxyl-mediated degradation.

4. Discussion

4.1. Catalyst physical properties

The method of doping TiO_2 with thiourea, as per Ohno's procedure is now well established and reproducible. Thiourea is a good source of nucleophilic sulfur; in organic synthesis, it is used as

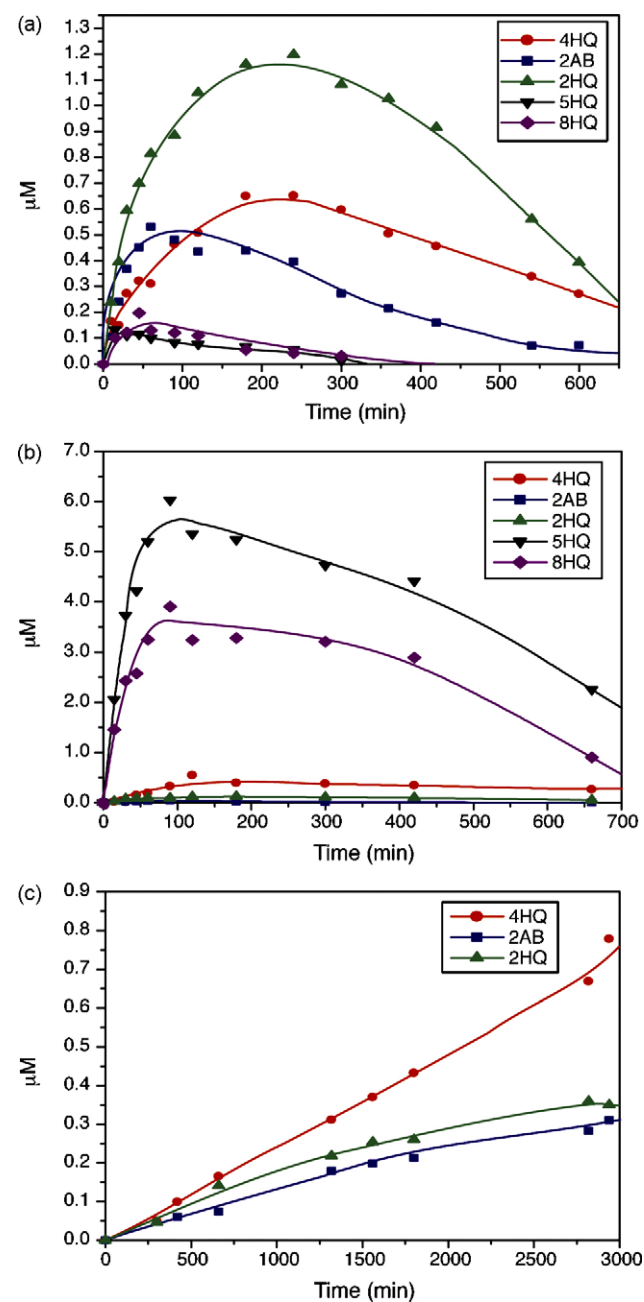


Fig. 8. Intermediate products formed from the S-TiO_2 -mediated degradation of quinoline at (a) pH 6 under 350 nm photolysis, (b) pH 3 under 350 nm photolysis, and (c) pH 6 under ≥ 495 nm.

a synthon for HS^- . (After initial reaction with an electrophile, a second step is usually used to hydrolyze the initial adduct and give urea as a byproduct.) To that extent, it is a sensible source of S for sol-gel preparations of TiO_2 . XPS data obtained before annealing (showing S^{2-}) are consistent with either thiourea as a physical mixture with the titania or with a covalent modification in which the oxidation state of sulfur has not changed. High temperature annealing under O_2 is necessarily oxidative, however, and S^{4+} and/or S^{6+} are what is observed thereafter. Since C and N are not detected by XPS, it is presumed that these are largely "burned off" by the high temperature annealing [35]. Indeed, Jin and co-workers showed through DSC measurements on similar preparations, that there is an exotherm near 220°C attributable to decomposition of urea/thiourea, and others near 265°C and 430°C attributed to

combustion of other organic substances [11]. It is also during the annealing process that the yellow color of the catalyst is developed, clearly indicating chemical incorporation of the S at this stage. The post-annealing spectra correspond to the sulfate oxidation state (or potentially SO_2), and suggest S-for-Ti substitution, as proposed by Ohno [13,15]. The etched XPS spectra show that the sulfur goes down at least several layers, though we presume it to be dispersed throughout.

The $\text{S}_8\text{-TiO}_2$ showed the same XPS data, save for a small S^{2-} peak after etching, which could suggest a minor fraction of S-for-O substitution. As with the Ohno-style, $\text{S}\text{-TiO}_2$, there could be a small amount of carbon also included in $\text{S}_8\text{-TiO}_2$; small amounts of residual solvent that remains after drying the material before the annealing. This is difficult to be certain of because the XPS for adventitious carbon adsorbed to the material from air overlaps strongly with the most likely resulting carbon product, i.e., coke condensation. (See ref [36].) The presence of small quantities of coke would also be consistent with the absorption tail that extends past 500 nm in the diffuse reflectance spectrum, as shown in Fig. 4. The differing annealing temperatures could account for the differing amounts of coke between $\text{S}_8\text{-TiO}_2$ and $\text{S}\text{-TiO}_2$, but to argue more specifically would be overly speculative.

The mechanism for incorporation of S in $\text{S}_8\text{-TiO}_2$ is uncertain. At this high temperature, initiation of sulfur chemistry by both homolysis and nucleophilic type attack is reasonable. The fact that the S remains in the XPS spectra after Ar-etching does imply that significant rearrangement of the surfaces and nearby layers occurs at this temperature, in that “penetration” of the sulfur in the TiO_2 is required by this result. Since the material generated by annealing with S_8 appears to be functionally equivalent to that generated by preparation with thiourea, it would seem there are advantages to preparing sulfur-doped TiO_2 in this manner: better optimization of the initial TiO_2 manufacture, and lower expense of the dopant. Optimization of the annealing step and/or use of other titania samples (e.g., P25) may result in a superior catalyst.

4.2. Photocatalytic results

The specifics of the oxidations of these three compounds, of course, are much less valuable than the generalities that can be drawn from them; these results must be placed in the context of various other types of physical studies, and we review the available literature to put the current results in context. At least for this set of probes, a consistent result was that degradation using UV light was slowed by the sulfur doping. This is similar to the observations of Sun, who also found an inverse relationship between activity in the visible and UV for C- and S-doped TiO_2 [11].

Apparently, contradictory arguments are made by various authors for the chemistry that should be derived from doped TiO_2 . These are manifest both in the explanation of kinetics and for the reactivity of the photogenerated holes. Consider, for example, the current observation that, under UV photolysis, $\text{S}\text{-TiO}_2$ always provided slower degradations than did TiO_2 .

Sun attributed the lower UV activity to S centers acting as recombination sites [11]. On the other hand, Tachikawa, based on flash photolysis experiments, concluded that S sites did not act as recombination centers [17]. By time-resolved diffuse reflectance spectroscopy (in acetonitrile or methanol), Majima and co-workers determined that the yield of charge carriers with 355 nm excitation is greater for undoped TiO_2 than for $\text{S}\text{-TiO}_2$ (made by the sol gel method with thiourea). However, the efficiency of hole transport to the surface is comparable for the two materials and the S-centers do not act as special recombination points [17]. The lower total number of charge separations naturally leads to a lower observed rate of disappearance.

On the other hand, mainly on the basis of efficiency measurements over a series of catalysts, Jin and co-workers conclude quite the opposite. They argue that the sulfur defects do act as recombination centers, and it is by this means that the UV efficiency is slightly lowered [11]. The current results do not settle this particular dispute. Instead, they reinforce the observation that this effect (that UV photocatalytic efficiency for the S-doped materials should be expected to be universally lowered, relative to the undoped case) is to be expected.

Thus, from a practical standpoint of optimizing a catalyst, the advantage or disadvantage of $\text{S}\text{-TiO}_2$ (in terms of speed of degradation) will depend entirely on the spectral distribution of the light source being used and the transmission of that light to the catalyst. The advantage of activity in the visible would have to make up for the loss of activity in the UV.

Therefore, to understand whether $\text{S}\text{-TiO}_2$ is an “improvement” over TiO_2 , knowing how universal and efficient the degradation initiated by visible irradiation is critical. If only certain substrates will be oxidized, and others untouched, its utility would certainly be limited to niche applications.

Given the model that main group dopants provide mid-gap filled orbitals, rather than changing the band structure of TiO_2 in a more fundamental way, an intuitive argument can be made that the S-centers represent “deep” h^+ traps, i.e., high energy orbitals from which electrons may fall. This should inherently lower the oxidizing power of the hole, relative to undoped TiO_2 assuming charge migration is faster than reaction with the organic substrate. The consequences of the “deep hole trapping”, however, remain a matter of discussion.

Majima and coworkers give a report that would be pessimistic regarding visible activity of their $\text{S}\text{-TiO}_2$ (also made by the Ohno method), at least in organic solvents. With 430 nm excitation, these authors report the formation of charge carriers, and formation of organic radical cations by direct irradiation of CT bands, but no SET oxidation of the organic adsorbate 4-(methylthio)benzyl alcohol after excitation [17].

Takeshita et al. contrasted the behavior of $\text{S}\text{-TiO}_2$ made by oxidative annealing of TiS_2 and by the Ohno method with thiourea [20]. Essential to their analysis was the observation that the sulfur remaining in the TiS_2 -based catalyst was largely in the center of the particle, with very little remaining in the exterior. This is in contrast to the sol-gel method, assumed to produce approximately homogeneously dispersed S. They argue, on the basis of flash photolysis experiments, that the sol-gel materials produce near-surface holes that are not capable of oxidizing water to produce HO^\bullet , but are able to oxidize methanol [20]. (This occurs whatever the excitation wavelength.) With the TiS_2 -based material, visible irradiation does not produce photoactivity, which is rationalized by assuming that the sulfur centers are deep within the particle and the charge carriers cannot migrate to the surface.

By contrast, for carbon-doped TiO_2 , Nakato reports that visible photooxidation of methanol goes by an indirect oxidation pathway functionally equivalent to $\text{HO}^\bullet_{\text{ads}}$ chemistry. This conclusion is based upon measurement of photocurrent in the presence and absence of methanol. Although the catalyst is not identical to the present case, the authors discuss the generality of this mechanism [7]. The chemical contrast, in that case, is that hydrogen abstraction of the C-H is the first step of methanol oxidation, rather than SET, followed by deprotonation, current doubling, and so on. In principle, this might be distinguished by means of competition experiments with isotope labeling, where the hydrogen abstraction should show a kinetic isotope effect.

Our method, instead, depends on a different chemical outcome by the two mechanisms, and indirect reasoning about the physical processes. The three probes used here each demonstrate a different pattern of reactivity, but can be assembled into a sensible whole.

4.2.1. Photocatalytic degradation of MR

The pH of 8.5 was chosen to study the “remediation” of MR because this was the pH at which degradation was the most efficient, and intermediates from both SET and hydroxyl chemistry had been observed [25]. Indeed, MR was degraded under these conditions more rapidly than either of the other probes. This is presumably attributable to both stronger adsorption [22] and a lower oxidation potential, though reversible oxidation potentials are not available for these compounds.

The most important result with MR, however, was the observation of both major oxidation pathways, even with visible light well to the red of the absorbance cutoff of TiO_2 . The chemistry occurring here could not result from the direct excitation of the undoped TiO_2 semiconductor since the light used here does not possess enough energy. We attribute this reactivity to the formation and direct irradiation of a charge transfer (CT) complex, which has been directly observed between phenol compounds and TiO_2 [32,33,37]. Although the intuitive expectation is for CT irradiation to result in chemistry essentially identical to normal SET chemistry, the work of Agrios and Gray shows wavelength dependence and multiple types of reactivity [33]. Indeed, we report a closely related phenomenon in Table 1, where the product ratios differ for the doped and undoped catalyst, presumably because some of the irradiation is direct to the catalyst in the case of S- TiO_2 . Although interesting as an independent phenomenon, this CT-based degradation does not significantly bear on whether S- TiO_2 will be a broadly useful catalyst, since only a subset of pollutants will form such CT complexes.

4.2.2. Photocatalytic degradation of AN

The degradation of AN with the Millenium Chemicals PC series, reported on previously [22], showed hydroxyl products dominating at neutral and higher pH. This is similar to the result reported for S- TiO_2 and UV irradiation in Table 1, but the total amount of observed intermediates was very small, in contrast, for undoped TiO_2 . The smaller quantities are consistent with secondary degradation that is faster than the first step.

Loss of AN mediated by either S- TiO_2 or TiO_2 with $> 495 \text{ nm}$ light was insignificant. While this is the expected result for TiO_2 , the S- TiO_2 shows modest absorption in this region and should be capable of generating charge carriers (and apparently does, given the results for quinoline). The lack of degradation of this molecule is thus reasonably damning to the prospects of S- TiO_2 as a versatile visible-light driven catalyst, at least this far into the visible. At least for this compound, both the SET and hydroxyl-like chemistry are shut down in the visible. The SET chemistry might be expected to be molecule-specific, i.e., that some more easily oxidized or better binding molecules might undergo SET even with the “weaker” holes due to the doping. However, though some controversy exists over the exact nature of the hydroxyl-like chemistry, it is widely believed to be “indirect”, in that an intermediate (TiO^\bullet , HO^\bullet , etc.) is produced that in turn reacts with the substrate. As AN is dominated by this chemistry in the UV, the lack of degradation of AN with lower energy light is strongly suggestive that the indirect oxidizing center is not formed.

4.2.3. Photocatalytic degradation of Q

The last probe, quinoline, leads to a variety of products under photocatalytic conditions, as a result of electronic demand differences in the benzene and pyridine rings. Pichat and co-workers showed that electrophilic hydroxyl radicals (e.g., Fenton conditions) favor addition to the benzene ring, and SET chemistry favors functionalization of the pyridine ring and formation of 2AB, 2HQ, and 4HQ [6]. The product distribution results reported here follow the trends of Pichat and co-workers, save for the differences in internal ratios of SET products, but as noted, we were able to

reproduce their results when using the same catalyst they did, i.e., P25.

Above the pKa of quinolinium, it is assumed that adsorption to the catalyst occurs largely through the nitrogen lone pair. At low pH, quinolinium is predominant and not as likely to adsorb to the also-positively-charged TiO_2 surface [38]. Not only does the poor binding suppress SET chemistry, but the protonation obviously increases the oxidation potential. We suggest that the approximate invariance in rate of degradation of Q with pH (Figs. 5 and 6) is merely coincidence.

Like AN, quinoline does not form a CT complex with TiO_2 that is degraded on visible excitation above the dark baseline, though trace 5HQ is observed at pH 3. (We presume that this is diagnostic of a very minor amount of hydroxyl chemistry that was simply undetected in the AN case.) Both 5HQ and 8HQ were observed with UV irradiation and TiO_2 (Fig. 7).

However, with S- TiO_2 , Q is significantly degraded by visible light at pH 6, if only through the SET pathways. Only SET products 2AB, 2HQ, and 4HQ (Fig. 8) are observed. We infer that the reactive holes in S- TiO_2 are able to oxidize quinoline, even if they are not able to do the same for AN.

5. Conclusion

Information on the mechanistic differences between S- TiO_2 and undoped TiO_2 was obtained through the use of three probe molecules. MR, AN, and Q each showed a different pattern of reactivity with respect to visible irradiation, with activity from both catalysts, neither catalyst, and only S- TiO_2 , respectively. The simplest interpretation of the results presented here is that S- TiO_2 , prepared by the Ohno method, does not produce active hydroxyl-like sites on excitation at $> 495 \text{ nm}$. Furthermore, the sulfur doping sites do act as deep hole traps that diminish the oxidizing power of the hole. Moreover, we observe, consistent with previous workers, that the UV activity of S- TiO_2 is somewhat diminished from its parent. As a result, the utility of S- TiO_2 over a broadly useful TiO_2 catalyst such as P25 will come when extension of the absorption spectrum into the visible is more important than efficient use of UV photons, and when the target pollutants are relatively easy to oxidize. It is generally the case that the early degradation steps – at least of aromatic type pollutants – make the resulting compounds easier to degrade by photocatalysis, so this latter restriction may not be as daunting as it might seem at first glance. It may also be useful as a component of a catalyst mixture designed to efficiently use the UV and also derive some activity from visible irradiation. Finally, due to the very similar results obtained for S- TiO_2 and S₈- TiO_2 (without significant optimization of the S₈ annealing step), and the ease of preparation and low cost of the sulfur atoms, the annealing of S₈ into extant TiO_2 catalysts (e.g., P25) may turn out to be an attractive approach.

Acknowledgement

The authors gratefully acknowledge the National Science Foundation (NSF CHE0518586) for support of this work, Prof. Clemens Burda for allowing us to obtain diffuse reflectance spectra on his instrument, Jim Anderegg for his assistance with XPS, and Brian Trewyn for obtaining TEM images and nitrogen sorption data.

References

- [1] (a) P. Pichat, Water Sci. Technol. 55 (2007) 167–173;
 (b) D.F. Ollis, H. Al-Ekabi, Photocatalytic Purification and Treatment of Water and Air, Elsevier Science Publishers, New York, 1993;
 (c) P.K.J. Robertson, D.W. Bahneemann, J.M.C. Robertson, F. Wood, Handbook of Environmental Chemistry 2 (2005) 367–423;

(d) A. Fujishima, X. Zhang, D.A. Tryk, *Surf. Sci. Reports* 63 (2008) 515–582;

(e) M. Kaneko, I. Okura, *Photocatalysis: Science and Technology*, Springer-Verlag, Berlin, 2002.

[2] J. Ryu, W. Choi, *Environ. Sci. Technol.* 42 (2008) 294–300.

[3] M.R. Hoffmann, S.T. Martin, W. Choi, D.W. Bahnemann, *Chem. Rev.* 95 (1995) 69–96.

[4] (a) T.L. Thompson, J.T. Yates Jr., *Chem. Rev.* 106 (2006) 4428–4453;

(b) M.A. Fox, M.T. Dulay, *Chem. Rev.* 93 (1993) 341–357;

(c) O. Legrini, E. Oliveros, A.M. Braun, *Chem. Rev.* 93 (1993) 671–698;

(d) J.S. Park, W. Choi, *Chem. Lett.* 34 (2005) 1630–1631.

[5] A.L. Linsebigler, G. Lu, J.T. Yates Jr., *Chem. Rev.* 95 (1995) 735–758.

[6] L. Cermenati, P. Pichat, C. Guillard, A. Albini, *J. Phys. Chem. B* 101 (1997) 2650–2658.

[7] H. Liu, A. Imanishi, Y. Nakato, *J. Phys. Chem. C* 111 (2007) 8603–8610.

[8] R. Asahi, T. Morikawa, T. Ohwaki, K. Aoki, Y. Taga, *Science* 293 (2001) 269–271.

[9] (a) M. Anpo, *Catal. Surv. Jpn.* 1 (1997) 169–179;

(b) W. Choi, A. Termin, M.R. Hoffmann, *J. Phys. Chem.* 98 (1994) 13669–13679;

(c) J.G. Highfield, P. Pichat, *New J. Chem.* 13 (1989) 61–66.

[10] (a) T. Umebayashi, T. Yamaki, S. Tanaka, K. Asai, *Chem. Lett.* 32 (2003) 330–331;

(b) H. Wang, J.P. Lewis, *J. Phys.: Condens. Matter.* 17 (2005) L209–L213;

(c) H. Wang, J.P. Lewis, *J. Phys.: Condens. Matter.* 18 (2006) 421–434;

(d) X. Wang, S. Meng, X. Zhang, H. Wang, W. Zhong, Q. Du, *Chem. Phys. Lett.* 444 (2007) 292–296;

(e) Y. Choi, T. Umebayashi, M. Yoshikawa, *J. Mater. Sci.* 39 (2004) 1837–1839;

(f) Z. Chen, G. Yu, P. Zhang, Z. Jiang, *Huanjing Kexue* 23 (2002) 55–59;

(g) X. Chen, C. Burda, *J. Phys. Chem. B* 108 (2004) 15446–15449;

(h) D. Chen, Z. Jiang, J. Geng, Q. Wang, D. Yang, *Ind. Eng. Chem. Res.* 46 (2007) 2741–2746;

(i) H. Irie, Y. Watanabe, K. Hashimoto, *Chem. Lett.* 32 (2003) 772–773;

(j) Y. Li, D.-S. Hwang, N.H. Lee, S.-J. Kim, *Chem. Phys. Lett.* 404 (2005) 25–29;

(k) J. Yang, H. Bai, X. Tan, J. Lian, *Appl. Surf. Sci.* 253 (2006) 1988–1994;

(l) K. Yang, Y. Dai, B. Huang, *J. Phys. Chem. C* 111 (2007) 12086–12090;

(m) S. Sakthivel, H. Kisch, *Angew. Chem. Int. Ed.* 42 (2003) 4908–4911;

(n) C. Xu, R. Killmeyer, M.L. Gray, S.U.M. Khan, *Appl. Catal. B* 64 (2006) 312–317;

(o) T.-h. Xu, C.-l. Song, Y. Liu, G.-r. Han, *J. Zhejiang Univ., Sci., B* 7 (2006) 299–303;

(p) T. Ohno, T. Tsubota, K. Nishijima, Z. Miyamoto, *Chem. Lett.* 33 (2004) 750–751;

(q) K.M. Reddy, B. Baruwati, M. Jayalakshmi, M.M. Rao, S.V. Manorama, *J. Solid State Chem.* 178 (2005) 3352–3358;

(r) Q. Zhang, J. Wang, S. Yin, T. Sato, F. Saito, *J. Am. Ceram. Soc.* 87 (2004) 1161–1163;

(s) T. Umebayashi, T. Yamaki, H. Itoh, K. Asai, *Appl. Phys. Lett.* 81 (2002) 454–456;

(t) D.B. Hamal, K.J. Klabunde, *J. Coll. Interf. Sci.* 311 (2007) 514–522;

(u) M. Katoh, H. Aihara, T. Horikawa, T. Tomida, *J. Coll. Interf. Sci.* 298 (2006) 805–809;

(v) W. Ho, J.C. Yu, S. Lee, *J. Solid State Chem.* 179 (2006) 1171–1176;

(w) S. Liu, X. Chen, *J. Haz. Mat.* 152 (2008) 48–55;

(x) M. Crisan, A. Braileanu, M. Raileanu, M. Zaharescu, D. Crisan, Dragan, M. Nicolae, A. Anastasescu, I. Ianculescu, V.E. Nitoi, S.M. Marinescu, Hodoregea, *J. Non-Crystalline Solids* 354 (2008) 705–711;

(y) S. Yin, M. Komatsu, Q.-w. Zhang, R.-x. Li, Q. Tang, F. Saito, T. Sato, *Guocheng Gongcheng Xuebao* 6 (2006) 477–481;

(z) Z. Zhou, X. Zhang, Z. Wu, L. Dong, *Chin. Sci. Bull.* 50 (2005) 2691–2695;

(aa) H. Li, X. Zhang, Y. Huo, J. Zhu, *Environ. Sci. Technol.* 41 (2007) 4410–4414;

(bb) S. Sato, *Chem. Phys. Lett.* 123 (1986) 126–128.

[11] H. Sun, Y. Bai, Y. Cheng, W. Jin, N. Xu, *Ind. Eng. Chem. Res.* 45 (2006) 4971–4976.

[12] (a) H. Irie, Y. Watanabe, K. Hashimoto, *J. Phys. Chem. B* 107 (2003) 5483–5486;

(b) S. Sakthivel, M. Janczarek, H. Kisch, *J. Phys. Chem. B* 108 (2004) 19384–19387;

(c) F. Tian, C. Liu, J. Phys. Chem. B 110 (2006) 17866–17871.

[13] T. Ohno, M. Akiyoshi, T. Umebayashi, K. Asai, T. Mitsui, M. Matsumura, *Appl. Catal. A* 265 (2004) 115–121.

[14] T. Ohno, T. Mitsui, M. Matsumura, *Chem. Lett.* 32 (2003) 364–365.

[15] T. Ohno, T. Tsubota, M. Toyofuku, R. Inaba, *Catal. Lett.* 98 (2004) 255–258.

[16] X. Yan, T. Ohno, K. Nishijima, R. Abe, B. Ohtani, *Chem. Phys. Lett.* 429 (2006) 606–610.

[17] T. Tachikawa, S. Tojo, K. Kawai, M. Endo, M. Fujitsuka, T. Ohno, K. Nishijima, Z. Miyamoto, T. Majima, *J. Phys. Chem. B* 108 (2004) 19299–19306.

[18] (a) C. Di Valentini, G. Pacchioni, A. Selloni, *Chem. Mater.* 17 (2005) 6656–6665;

(b) V.N. Kuznetsov, N. Serpone, *J. Phys. Chem. B* 110 (2006) 25203–25209.

[19] T. Tachikawa, Y. Takai, S. Tojo, M. Fujitsuka, H. Irie, K. Hashimoto, T. Majima, *J. Phys. Chem. B* 110 (2006) 13158–13165.

[20] K. Takeshita, A. Yamakata, T. Ishibashi, H. Onishi, K. Nishijima, T. Ohno, *J. Photochem. Photobiol. A: Chem.* 177 (2006) 269–275.

[21] (b) J. Tschirch, D. Bahnemann, M. Wark, J. Rathousky, *J. Photochem. Photobiol. A* 194 (2008) 181–188;

(b) J. Tschirch, R. Dillert, D. Bahnemann, B. Proft, A. Biedermann, B. Goer, *Res. Chem. Int.* 34 (2008) 381–392.

[22] T. Hathway, W.S. Jenks, *J. Photochem. Photobiol. A* 200 (2008) 216–224.

[23] (a) R. Enriquez, A.G. Agrios, P. Pichat, *Catal. Today* 120 (2007) 196–202;

(b) H. Kominami, S. Murakami, J. Kato, Y. Kera, B. Ohtani, *J. Phys. Chem. B* 106 (2002) 10501–10507.

[24] M. Ranchorella, C. Rol, G.V. Sebastiani, *J. Chem. Soc. Perkin Trans 2* (2000) 311–315.

[25] X. Li, J.W. Cubbage, W.S. Jenks, *J. Photochem. Photobiol. A* 143 (2001) 69–85.

[26] L. Cermenati, A. Albini, P. Pichat, C. Guillard, *Res. Chem. Intermed.* 26 (2000) 221–234.

[27] C. Lang'at-Thorwua, T. Song Tong, J. Hu, L. Simons Andrean, A. Murphy Patricia, *J. Nat. Prod.* 66 (2003) 149–151.

[28] X. Li, J.W. Cubbage, T.A. Tetzlaff, W.S. Jenks, *J. Org. Chem.* 64 (1999) 8509–8524.

[29] (a) W.D. Bowman, J.N. Demas, *J. Phys. Chem.* 80 (1976) 2434–2435;

(b) C.G. Hatchard, C.A. Parker, *Proc. Royal. Soc. A* 235 (1956) 518–536.

[30] (a) J.F. Moulder, W.F. Stickle, P.E. Sobol, K.D. Bomben, *Handbook of X-Ray Photoelectron Spectroscopy*, Perkin-Elmer Corporation (Physical Electronics): Eden Prairie, MN, 1992;

(b) D.I. Sayago, P. Serrano, O. Bohme, A. Goldoni, G. Paolucci, E. Roman, J.A. Martin-Gago, *Phys. Rev. B* 64 (2001) 205402/1–205402/7;

(c) D.I. Sayago, P. Serrano, O. Bohme, A. Goldoni, G. Paolucci, E. Roman, J.A. Martin-Gago, *Surf. Sci.* 482–485 (2001) 9–14;

(d) E. Roman, J.L. De Segovia, J.A. Martin-Gago, G. Comtet, L. Hellner, *Vacuum* 48 (1997) 597–600.

[31] The rates are not quantum yields; no attempt was made to quantify the fraction of light absorbed.

[32] S. Kim, W. Choi, *J. Phys. Chem. B* 109 (2005) 5143–5149.

[33] (a) A.G. Agrios, K.A. Gray, E. Weitz, *Langmuir* 19 (2003) 5178;

(b) A.G. Agrios, K.A. Gray, E. Weitz, *Langmuir* 20 (2004) 5911–5917.

[34] C. Richard, *New J. Chem.* 18 (1994) 443–445.

[35] Small amounts of “atmospheric” carbon are always detected by XPS; we cannot eliminate the possibility of small amounts of graphitic type carbon in the final catalyst.

[36] E.M. Rockafellow, X. Fang, B.G. Trewyn, K. Schmidt-Rohr, S. Jenks William, *Chem. Mater.* 21 (2009) 1187–1197.

[37] A. Orlov, D.J. Watson, F.J. Williams, M. Tikhov, R.M. Lambert, *Langmuir* 23 (2007) 9551–9554.

[38] Due to analytical difficulties the Pichat group was unable to quantify 8HQ, but we were able to separate this material chromatographically from the others.